Scientia Iranica B (2023) 30(5), 1548–1561

Sharif University of Technology
Scientia Iranica
Transactions B: Mechanical Engineering
http://scientiairanica.sharif.edu

An overall grasp evaluation function to evaluate and optimize prosthetic hands

H. Sayyaadi* **and S.R. Homam**

School of Mechanical Engineering, Sharif University of Technology, Tehran 11155-9567, Iran.

Received 19 January 2022; received in revised form 4 October 2022; accepted 28 November 2022

KEYWORDS
prosthetic hand;
Grasp quality;
Optimization;
Hand kinematics;
Robotics.

Abstract. Since weight limitation on prosthetic hands limits their actuator numbers, designers cannot bio-mimic human hand. Therefore, optimization is required in order to develop prosthetic hands that could mimic the human hand performance as close as possible despite limitations. Hence, the objective function is to correlate the configuration of prosthetic hands to their performance in terms of their ability to grasp various objects like the human hand. The assessment was done by evaluating an accessible workspace and a grasp quality index. Forward kinematics was implemented to grade the workspace. Grasp ability was measured using the volume of the grasp wrench space, one of the grasp quality indexes. The grasp quality cannot rate prosthetic hands solely. As a result, techniques including randomization and grasp taxonomy were employed. Further, the function was applied to specify the importance of each finger and the Degree of Freedom (DOF) of the human hand. The results show that the most significant finger is the thumb. The most crucial DOFs are the abduction movement of the thumb's carpometacarpal (CMC) joint and the index's metacarpophalangeal (MCP) joint. Finally, the optimized configuration is proposed using the Taguchi method.

1. Introduction

Human hand performs vital tasks, namely grasping objects and manipulating abilities. Overall, it enables interacting with our surroundings and experiencing physically. Loss of this vital organ results in significant functionality loss, and prosthetic hands are employed to restore the human hand function. However, since the human hand has a significant Degree of Freedom (DOF) (in this research, DOFs are joint movements that are shown in Table 1) as high as 26 [1] in a dense space, designing fine end effectors and prosthetic hands is difficult to achieve.

Different industrial hands try to imitate the human hand. One of the best examples is the 4.3 kg Shadow hand [2]. It can grasp and manipulate objects superbly through 20 actuated DOFs.

Although Shadow hand is of perfect performance, it is an unfit prosthesis since it weighs 4.3 kg. The human hand weight is around 400 g [3]; thus, the weights of commercially available prosthetic hands are close to this quantity [4]. The difference between the human hand and shadow hand weight shows the limitation that prosthetic hands deal with, affecting the number of actuators they can have.

In this study, the configuration of a prosthetic hand is the framework that specifies which human hand DOFs are driven by which actuators and which ones are

*. *Corresponding author.*
E-mail addresses: sayyaadi@sharif.edu (H. Sayyaadi); homamreza@gmail.com (S.R. Homam)

doi: 10.24200/sci.2022.59779.6418

Table 1. Association of each DOF with a number.

Finger	Thumb (I)				Index (II)				Middle (III)	
Joint	CMC		Metacarpophalangeal (MCP)	Interphalangeal (IP)	MCP		PIP	DIP	MCP	
Movement	Ab/Ad[a]	F/E[b]	F/E	F/E	Ab/Ad	F/E	F/E	F/E	Ab/Ad	F/E
Joint number	1	2	3	4	5	6	7	8	9	10
Finger	**Middle (III)**		**Ring (IV)**				**Little (V)**			
Joint	**PIP**	**DIP**	**MCP**		**PIP**	**DIP**	**MCP**		**PIP**	**DIP**
Movement	F/E	F/E	Ab/Ad	F/E	F/E	F/E	Ab/Ad	F/E	F/E	F/E
Joint number	11	12	13	14	15	16	17	18	19	20

Note: [a]Ab/Ad = Abduction/Adduction; [b]F/E = Flexion/Extension.

Table 2. Hand configurations from different research studies.

Joint number	1	2	3	4	5	6	7	8	9	10	11	12	13	14	15	16	17	18	19	20
Hand models																				
OLYMPIC [14]	0.5	0.5	1	1	0	2	2	2	0	3	3	3	0	4	4	4	0	5	5	5
Version 1 [5]	0.5	0.5	1	1	0	1	1	0	0	1	1	0	0	1	1	0	0	1	1	0
Version 2 [5]	0	0	1	0	0	1	1	0	0	1	1	0	0	1	1	0	0	1	1	0
[16]	1	1	1	1	0	2	2	2	0	3	3	3	0	3	3	3	0	3	3	3
Galileo hand [10]	1	1	2	2	0	3	3	3	0	4	4	4	0	5	5	5	0	6	6	6
CORA hand [11]	1	1	2	2	0	3	3	0	0	4	4	0	0	5	5	0	0	6	6	0
[15]	0	0	1	1	0	2	2	0	0	3	3	0	0	3	3	0	0	3	3	0
MERO Hand [17]	1	1	2	2	0	2	2	2	0	2	2	2	0	2	2	2	0	2	2	2
SSSA-MyHand [7]	1	1	2	0	0	3	3	0	0	4	4	0	0	4	4	0	0	4	4	0
Lightweight Delft Cylinder Hand [18]	0	0	0	0	0	1	1	0	0	1	1	0	0	1	1	0	0	1	0	0
F3Hand [6]	0.5	0.5	1	1	0	1	1	1	0	1	1	1	0	1	1	1	0	1	1	0
[12]	1	1	2	2	3	4	4	4	0	5	5	5	3	6	6	6	3	7	7	7
SensorHand (2009) [4]	0	0	1	0	0	1	0	0	0	1	0	0	0	0	0	0	0	0	0	0
Vincent Hand (2010) [4]	1	1	2	2	0	3	3	0	0	4	4	0	0	5	5	0	0	6	6	0
Bebionic (2011) [4]	0.5	0.5	1	1	0	2	2	2	0	3	3	3	0	4	4	4	0	5	5	5
Michelangelo (2012) [4]	1	1	2	0	0	2	0	0	0	2	0	0	0	0	0	0	0	0	0	0
[9]	0.5	0.5	1	1	0.5	1	1	1	0.5	1	1	1	0.5	1	1	1	0.5	1	1	1

motionless. This study models the human hand with 20 DOFs. Their location within the hand and their associated number are given in Table 1.

Various prosthetic hands with different configurations have been developed so far. Some studies have managed to reduce the hand weight employing artificial muscles [5,6]. In [5] have introduced two different versions. The difference is that the first version has a manually movable carpometacarpal (CMC) joint of the thumb, whereas the second version makes the joint static. Both versions make distal interphalangeal (DIP) joints of the fingers stationary. On the contrary, F3Hand [6] activates all the DIP joints except the little finger. SSSA-My Hand [7] uses the Geneva mechanism to generate two semi-independent DOFs using one actuator, thus reducing the number of actuators. Another approach to keeping prosthetic hands light in weight is using only one actuator [8,9]. Although several designers are aware of the critical role of the thumb and use two actuators for the thumb, one for the Flexion/Extension (F/E) and the other for the opposition movements [10–13], or by having one motor for F/E and enabling opposition movement manually [14], other studies did not consider any movement for the opposition moment [15]. The difference in the findings of various relevant research articles is shown in Table 2, which involves the description of prosthetic hand configurations. In Table 2, each joint movement is represented by a number, as described in Table 1. '0' indicates that the associated joint is stationary in each configuration; '0.5' means that it is movable manually; and other DOFs with the same number are driven and coupled to each other.

Numerous studies have categorized how the hu-

man hand grasps things to comprehend the complexity of the grasping process. A study identified ways that Split-Hook Prosthetic Devices could grasp objects and present grasp taxonomy based on the grasp shape and force exertion [19]. Another study obtained the taxonomy of continuum robots [20]. In addition, many research studies have developed grasp taxonomy for the human hand; for instance, the study in [21] introduced grasp types in manufacturing tasks. In [22], 22 taxonomies were analyzed and 33 grasp types were obtained as a result. Grasp taxonomy is a powerful tool since it can be applied to grasp synthesis problems. In [23], grasp synthesis of the human hand with different shaped objects was implemented.

Grasp taxonomy can be employed to propose an optimal hand configuration. In one study, the movement of hand joints doing different grasps was captured and analyzed by correlations and adaptability to determine which movements were most important to be actuated more independently [24]. Similarly, Zarzoura et al. [25] analyzed the movement of hand joints doing different activities on a daily basis and further studied which joints could be described more with other joints and, as a result, can be actuated in one group. None of these two studies introduced an evaluation function. In another research, different fingertip poses in different grasping cases were captured. Then, nonlinear dimensionality reduction was used to represent all fingertip poses in a two-dimensional space. The grade calculates the overlap between the two-dimension space of the human hand and the artificial hand [26]. In these studies, hand configuration was studied by focusing on the workspace, but did not consider how firmly they could grasp objects. To address this issue, one study examined and categorized different grasp types and decided how many grasp types each hand configuration could achieve [27]. This research cannot decide how firm a specific hand configuration grasps objects via different grasp types.

Therefore, limitations on prosthetic hands challenge designers to develop prosthetic hands as functional as the human hand. As a result, it is crucial to introduce an evaluation function to evaluate or optimize hand configurations.

Hence, this research aims to propose an evaluation function connecting hand configuration to its performance. The function can make the tradeoff between functionality and weight clearer. Furthermore, it is employed to guide designers and to generate an optimal hand configuration using the Taguchi method. It is employed to cope with statistical numbers.

Section 2 discusses how the evaluation function assesses prosthetic hands. Section 3 introduces results comparable to other studies, explores the importance of different hand sections, and generates one optimal hand configuration. Section 4 gives a discussion on the results. Finally, Section 5 introduces the conclusion and future work.

2. Overall functionaly evaluation

Human hand can grasp various objects of different sizes and properties. The grasp consists of three phases: pre-grasp, grasp, and post-grasp. At the pre-grasp phase, prosthetic hands pose with respect to target objects, and grasp is when prosthetic hands hold objects firmly in that specific pose. Moreover, post-grasp is the manipulation phase [28].

The full functionality of the human hand cannot be duplicated with prosthetic hands because of their current limitations. Therefore, for evaluation, pre-grasp and grasp phases will be considered only and the manipulative skills will be omitted.

Based on the above definition, the responsibility of the moving parts of the prosthetic hands is to have a great workspace to grasp objects of different sizes and have a good grasp quality to grip them firmly.

2.1. Human hand model

The human hand is modeled so that it can be applied as an ideal benchmark. Also, to evaluate the differences between hand configurations and curb other differences, all hand configurations have the exact dimensions as the human hand model.

The human hand proposed in this research is modeled with 20 DOFs, as listed in Table 2. This research does not consider several DOFs, namely Abduction/Adduction (Ab/Ad) of the Metacarpophalangeal (MCP) and IP joints of the thumb, because they were considered stationary in [29]. In addition, movements of the fingers' CMC joints besides the thumb provide great stability than mobility [29]. According to this research [30], all the necessary data for modeling the human hand were measured and represented by two factors, namely Hand Length (Hl) and Hand Breadth (HB). The 25-DOF human hand model proposed in [31] applied the measured data in [30]. Similarly, this research employed that data to model the hand model. At first, the mean of two factors was obtained from [32] ($HL = 18.49$ cm, $HB = 8.42$ cm). Next, Denavit-Hartenberg parameters of the individual fingers were established using the dimensions of different segments of fingers, as Figure 1 depicts. $L_{i,j}$ represent segment dimensions, where i indicates the finger number and j is the length between different joints. The global coordinate lies in the wrist of the human hand, and the position of Ab/Ad of individual fingers with respect to the global coordinate is measured [30].

Having upper and lower limits for each joint movement is necessary to study a suitable workspace. This research was inspired by the findings in [33,34]. All the necessary data were not included in those

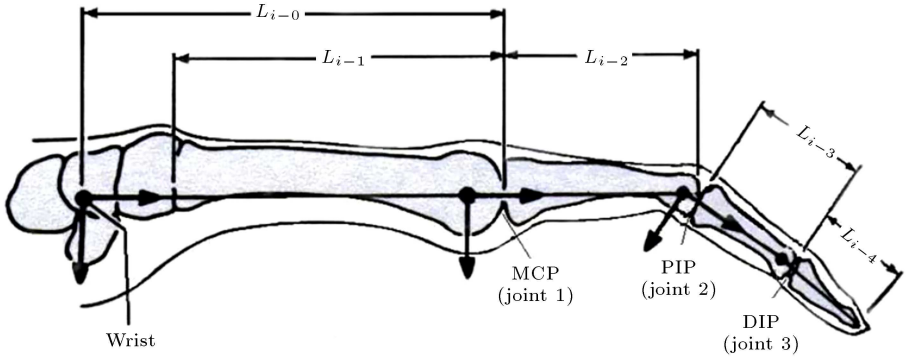

Figure 1. Length between joints in one finger [31].

references. As a result, some assumptions like the values of initial angles of DIP fingers were presumed.

2.2. Workspace evaluation

In order to quantify workspace, the volume of accessible workspace for each fingertip position is calculated and the grade is the summation of the finger volume. Since the volume is calculated for each fingertip separately, if one motor drives two joints from different fingers, it only is considered to participate in forming a workspace of one finger.

This paper used the discretization method given in [35] to form a workspace and calculate its volume. At first, the joint space is discretized into a finite set of points. Afterward, each point in the joint space transforms into the 3D workspace. For example, H_{ijk} is one of the points in the workspace, as shown in Figure 2. Next, the workspace is discretized such that each voxel has a dimension of $\Delta x \times \Delta y \times \Delta z$. Therefore, it could be represented in a binary 3D matrix where each element stands for each voxel. When the element is number 1, it means that the corresponding voxel is part of the workspace; if the number is zero, the voxel is not part of the workspace.

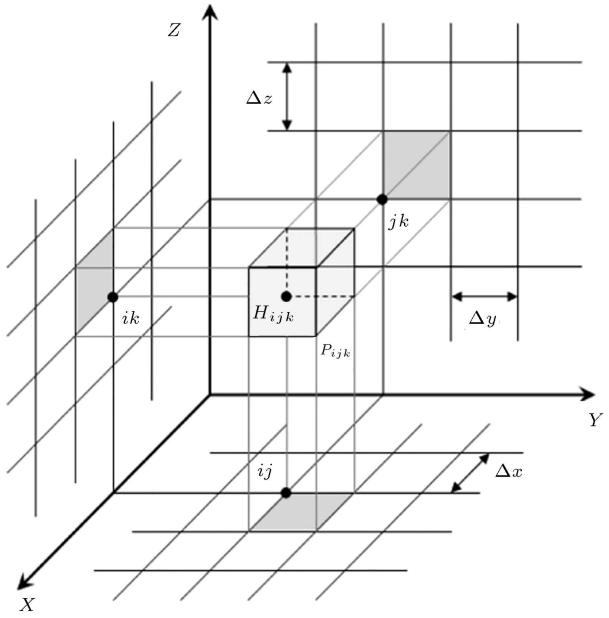

Figure 2. Discretizing workspace into voxels [35].

2.3. Grasp quality evaluation

In [36], various grasp quality indexes were reviewed. Among them, "Volume of the Grasp Wrench space" [37] was chosen because it calculated how well a grasp could resist external perturbation wrenches in any direction.

To calculate the index, contact points and their normal directions between a hand and an object being grasped must be specified. Then, according to the Coulomb friction model, there is a friction cone in each of n contact points. Each friction cone is approximated with an m-sided pyramid. Wrenches are established, which are given by Eq. (1):

$$\omega = \begin{pmatrix} f_{i,j} \\ \alpha(d_i \times f_{i,j}) \end{pmatrix}, \tag{1}$$

where $f_{i,j}$ is one of the m forces at the contact i, d_i is the vector from the torque origin to the ith point of contact, and α is the multiplier that matches units of torque to units of force. Next, the grasp wrench space is calculated by Eq. (2):

$$\begin{aligned} &grasp\ wrench\ space = \\ &\quad Convex\ Hull(\bigcup_{i=1}^{n} \{\omega_{i,1}, ..., \omega_{i,m}\}). \end{aligned} \tag{2}$$

Finally, the volume of the wrench can be calculated as an index. A more detailed procedure is available for further information in [37].

As a result, various inputs are required to evaluate the grasp quality, as listed in Figure 3. Being ideal for grasp planning, grasp quality indexes only measure the quality of one object with specific contact locations. In order to modify the grasp quality to be suitable for evaluating hand configurations, these requirements should be reformulated. As a result, for modifications, some techniques are given in this paper, as presented in Figure 3. The details of these techniques are shown in the following.

The first requirement is the need for a specific

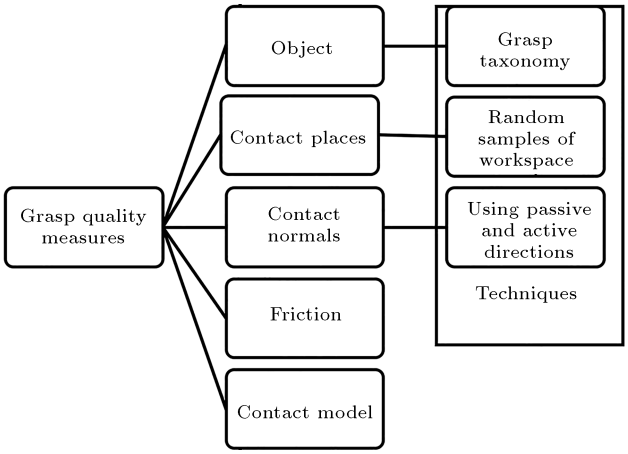

Figure 3. Five requirements for calculating the grasp quality. Three techniques that generalize the grasp quality.

object. Grasp taxonomy represents all the grasping methods and curbs the need to use one specific object. In [22], 33 grasp types were identified, as listed in Table 3. With the help of data, categorization made in [22], and the 3D models of grasps (provided online at http://grasp.xief.net), this research determines Phalanges that have a role in each grasp type and their applied force directions, as shown in Table 3. Since objects are omitted from this work, contacts are placed in prosthetic hands. Besides, as shown in Table 4, grasps with duplicate contact features are grouped as one, and the frequency of their usage is written. Four rows did not count as groups because their frequency of usage is zero or they have only two contact points.

Another input is the contact places. The grade of the grasp quality index differs when the contact places change. Hence, the grasp quality should be calculated in the accessible workspace of the prosthetic hand and an average score is calculated to realize the general ability of the prosthetic hand. Since evaluating the prosthetic hand in the workspace is time-consuming, this research selects uniformly distributed random points from the workspace and examines only those points. These random samples represent all the workspace and add uncertainty to the evaluation number.

Another step in Figure 3 is to specify contact forces. Since there are no objects to form the direction of contact forces and the grasp evaluation must represent the general ability of the hand configuration, force directions must differ from the conventional approach. The procedure used in this research is that active force directions of phalanges listed in Table 3 based on grasp types are identified. Active force directions are obtained in phalanges using the hand Jacobian matrix to obtain directions on which the prosthetic hand can exert force. Suppose that angles between all active force directions in a phalange and its ideal contact direction (specified in Table 3 as p or s) are equal to or more than 90 degrees. In this case, those active forces will not participate in grasping, since no active direction combination in the phalange could form a force in the desired direction. Besides active forces, passive forces are directions in the prosthetic hand that can withstand external forces, but since they are passive, they must be excited at first. In the next stage, the directions that can withstand or generate forces in phalanges having a rule are formed, which are called structural forces in this research. Then, the wrenches of those structural forces and active forces are obtained. In the subsequent stage, if the structural wrenches are not force closure, the grasp quality is zero. Otherwise, the grasp quality is calculated by the convex hull of the active wrenches and passive wrenches. Since the structural grasp is force closure, if one motor is activated, one wrench can be generated to oppose that activated wrench; these are the passive wrenches that participate in examining that grasp.

2.4. Assumptions

This research considers the following assumptions:

Assumption (1): The human hand was modeled with 20 DOFs, and the palm and wrist movements were not considered in this research;

Assumption (2): Objects were not used in the research. Instead, random samples of the workspace of prosthetic hands were generated. This method was applied to maintain the generality and represent grasp quality in the whole workspace rather than being restricted to several objects;

Assumption (3): Contacts were assumed to be in the middle of segments except for the last segment of fingers (distal phalanges), which were placed at the tip of fingers;

Assumption (4): This research employed the Coulomb friction point contact model; thus, two-point contacts could not be regarded as force closure grasps;

Assumption (5): Friction cones were approximated with four forces;

Assumption (6): Segments with a rule in each grasp type were established, as shown in Table 3. However, rules of segments might be established in different manners;

Assumption (7): Friction coefficient was set to 0.4.

Two algorithms proposed in this research were used to implement relevant concepts in the workspace evaluation and grasp quality evaluation subsections to evaluate hand configurations. The first algorithm developed a mathematical model to describe a prosthetic hand, to be used further in the second algorithm. The

Table 3. Description of segments involved in each grasp type. Segments that have letters "p" or "s" are engaged in that specific grasp. "p" and "s" indicate that the required force direction is achieved using the pad and the side of the segment, respectively. Numbers 1, 2, 3, and 4 in all the fingers except thumb are metacarpals, proximal phalanges, middle phalanges, and distal phalanges, respectively. Numbers 1, 2, and 3 in thumb are metacarpal, proximal phalange, and distal phalange, respectively.

	Finger	**Thumb**			**Index**				**Middle**				**Ring**				**Little**			
Grasp type	**Segment**	**1**	**2**	**3**	**1**	**2**	**3**	**4**	**1**	**2**	**3**	**4**	**1**	**2**	**3**	**4**	**1**	**2**	**3**	**4**
1	Large diameter	p	p	p	p	p	p	p	p	p	p	p	p	p	p	p	p	p	p	p
2	Small diameter	p	p	p	p	p	p	p	p	p	p	p	p	p	p	p	p	p	p	p
3	Medium wrap	p	p	p	p	p	p	p	p	p	p	p	p	p	p	p	p	p	p	p
4	Adducted thumb	p	p	p	p	p	p	p	p	p	p	p	p	p	p	p	p	p	p	p
5	Light tool			p		p	p	p		p	p	p		p	p	p		p	p	p
6	Prismatic 4 finger			p			p	p				p				p				p
7	Prismatic 3 finger			p			p	p				p				p				
8	Prismatic 2 finger			p			p	p				p								
9	Palmar pinch			p				p												
10	Power disk	p	p	p	p	p	p	p	p	p	p	p	p	p	p	p	p	p	p	p
11	Power sphere	p	p	p	p	p	p	p	p	p	p	p	p	p	p	p	p	p	p	p
12	Precision disk			p				p				p				p				p
13	Precision sphere			p				p				p				p				p
14	Tripod			p				p				s								
15	Fixed hook				p	p	p	p	p	p	p	p	p	p	p	p	p	p	p	p
16	Lateral			p			s	s												
17	Index finger extension			p				p	p	p	p	p	p	p	p	p	p	p	p	p
18	Extension type			p	p			s				s				s	p			s
19	Distal type		p			p				p				p					p	
20	Writing tripod			p	s			p				s								
21	Tripod variation			p	s			p				s				s				
22	Parallel extension			p		p	p	p		p	p	p		p	p	p		p	p	p
23	Adduction grip						s				s									
24	Tip pinch			p				p												
25	Lateral tripod	p		p				p			s									
26	Sphere 4 finger	p	p	p	p	p	p	p	p	p	p	p	p	p	p	p				s
27	Quadpod			p				p				p				p				
28	Sphere 3 finger	p	p	p	p	p	p	p	p	p	p	p			s					
29	Stick			p			s		p			p	p			p	p			p
30	Palmar	p	p		p			p	p			p	p			p	p			p
31	Ring		p	p	p	p	p	p												
32	Ventral			p			s		p			p	p			p	p			p
33	Inferior pincer			s			p													

second algorithm evaluated the overall functionality of the prosthetic hand.

The first algorithm takes a hand configuration as an input, as depicted in Figure 4, and by using the Denavit-Hartenberg parameters for each finger, transformation matrices for each segment are made. Afterward, global positions of contact points are formed using transformation matrices and local positions of contact points. Then, the linear velocity is obtained by taking the derivative of the positions. Next, Jacobian matrices are made by partial derivative of velocities with respect to joint velocities. Finally, the matrices

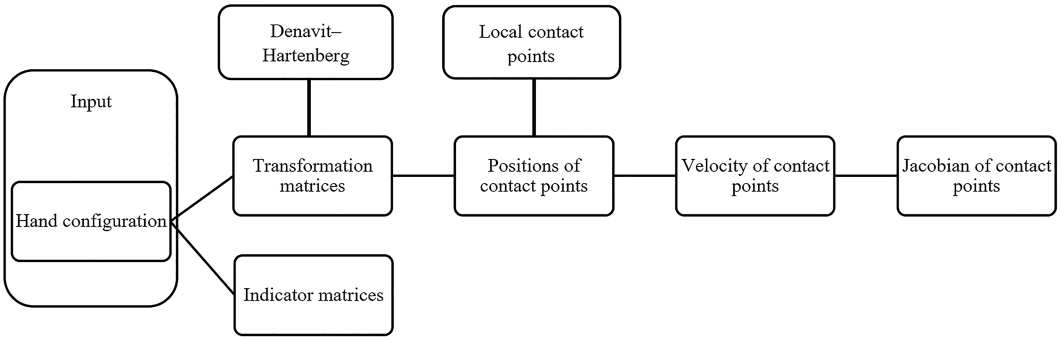

Figure 4. Stages of the first algorithm.

Table 4. Grasp types grouping and their frequency of usage. The frequency of each grasp type is reported from [22] and the frequency of each grasp number is the total frequency of all the associated grasp types.

Grasp number	Grasp types	Frequency (%)
1	1,2,3,4,10,11	22.6
2	5,22	6.8
3	6	4
4	7	4.2
5	8	6.4
	9,24	4.2
6	12,13	7.3
7	14	8.4
8	15	0.4
9	16	8.9
10	17	3.4
11	18	3.6
	19	0
12	20	0.7
	21	0
	23	2.2
13	25	10.4
14	26	0.2
15	27	0.3
16	28	1.5
17	29,32	1.6
18	30	0.6
19	31	0.2
	33	0.6

formed from hand configurations are employed to indicate which transformation and Jacobian matrices are connected to which actuators and segments.

Algorithm 1 is for calculating kinematics model of prosthetic hand and Algorithm 2 for performance assessment of prosthetic hand, which consists of three parts. The first part assesses the workspace. Each finger has a 3D binary matrix (*workspace-matrix*$\{j\}$) representing the fingertip workspace. A possible joint space of the finger is established, and the associated fingertip positions are formed (m). Next, their correlated voxels in the workspace-matrix element become 1. Finally, the workspace grade is the sum of all workspace-matrix elements (*Workspace-Grade*).

In the second part, random samples of the joint space are generated ($x\{j\}$). In the last part, the grasp quality of 19 grasp numbers (*Grasp-Grade*) in Table 4 is computed. At first, active and structural forces are derived (*active-forces, structural-forces*). Active forces can be found through Jacobian matrices. Structural forces can be formed based on the segments and their ideal contact location. Then, directions within minus 90 to 90 degrees of the ideal contact directions are considered structural forces. Next, if the wrench of the structural forces is force closure, it means that one opposing force of active forces can be generated for each motor. Then, the wrench of active and opposing forces is formed and is stored in a variable called grasp wrench. In case that grasp wrench is force closure, the volume of the convex hull is added to the corresponding grasp number (*Grasp-Grade*$\{j\}$).

These algorithms give an insight into how well a specific configuration of a prosthetic hand can deal with various object shapes and sizes (*Workspace-Grade*) and how well it grasps using different grasping methods (*Grasp-Grade*). Moreover, they are used for optimization purposes in which the fitness function would be one of the grades, separately or in combination. One possible combination used in this research is that each grasp number grade is multiplied by its weighting parameters, which are the frequency of usage listed in Table 4. The summation of those scores, called the overall grasp grade (*Overall-Grasp-Grade*), is then multiplied by the workspace grade (*Overall-Functionality-Grade*). It should be noted that the workspace and grasp grades for the human hand are computed 20 times, and the mean value of those is employed by which all the workspace grades and grasp grades are divided. It is implied that they are all normalized; hence, the best score is one.

```
DH = Denavit–Hartenberg for every finger
HC = hand configuration
CP = Local position of contact points
for each finger: i = 1 : 5 do
   for each segment j = 1 : 3 do
      T {i} {j} = Forming the transformation matrix by using HC and DH
      V {i} {j} = Calculating the velocity of contact points by using T and CP
      J {i} {j} = Generating the Jacobian by using T
   end for
end for
```

Algorithm 1. Generating the mathematical model of prosthetic hands.

```
for each finger: j = 1 : 5 do
   workspace-matrix{j} = 3D zero matrix
# n_{k,j} is the number of all discretized points in finger j
   for each discretized point in the joint space: k = 1 : n_{k,j} do
      m = fingertip position of k joint angles via transformation matrices
      p = index of the voxel that is associated with the m
      workspace-matrix{j}{p} = 1
   end for
end for
Workspace-Grade = summing of all the Workspace-matrix elements
n_s = sample number of the workspace
for each space: j = 1 : n_s do
   x{j} = random joint space based on the indicator matrices
end for
for each grasp number: j=1 : 19 do
   Grasp-Grade{j} = 0
   for each joint space: k = 1 : n_s do
      p = index of the directions that have a rule based on the j and indicating matrices
      active-forces = jacobian{x{k}}{p}
      structural-forces = developing based on the j and x{k}
      if wrench (structural-forces) is force closure do
         omitting contact points in active-forces that cannot produce ideal contact directions
         active-wrench = wrench (active-forces)
         opposing-wrench = forming wrenches opposite of active-wrench for each motor
         grasp-wrench = [active-wrench opposing-wrench]
         if grasp-wrench is force closure do
            pc = ConvexHull (grasp-wrench)
            Grasp-Grade{j} = Grasp-Grade{j} + volume (pc)
         end if
      end if
   end for
end for
Overall-Grasp-Grade = Σ (freq_j × Grasp-Grade{j})
Overall-Functionality-Grade = Workspace-Grade × Σ (freq_j × Grasp-Grade{j})
```

Algorithm 2. Performance assessment of prosthetic hands.

3. Results

As Algorithm 1 indicates, workspace grades are definite and grasp grades are statistical numbers. As a result, the overall grasp and functionality grades are statistical numbers. The code had 100 samples (*ns* in Algorithm 1) except for evaluating the importance of DOF (Table 5), which was 200. Then, for each grade, the code ran 20 times. Then, 20 calculated numbers of grades were analyzed through one-way ANOVA (Analysis of Variance). Eventually, we implemented the post hoc Tukey method [38]. The codes and more detailed results can be found in [39].

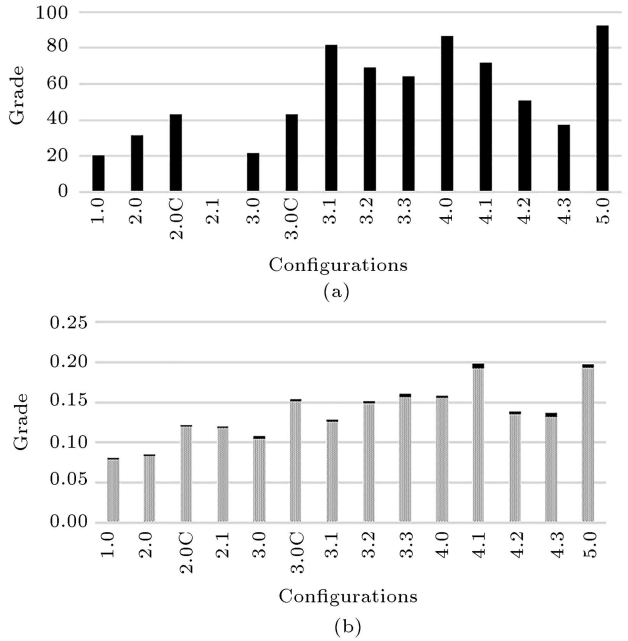

Figure 5. Assessment of hand configurations via (a) grasp functionality [27] and (b) overall grasp grade. In random data, the solid black color indicates a 95% confidence interval.

3.1. Comparison of evaluation function with other studies

In [27,40], some hand configurations were examined, as shown in Figures 5(a) and 6(a). The first digit of each configuration number represents the number of actuators it has. The remaining digits and letters were used to differentiate between configurations with the same number of actuators and another. The full description of those configurations was addressed in [27,40]. Assessment of those configurations was examined by our evaluation function: Workspace grade, overall grasp grade, and overall functionality grade, as shown in Figure 5(b), Figure 6(b), and Figure 6(c), respectively. It is better to compare Figure 5(a) with Figure 5(b) as well as Figure 6(a) with Figure 6(b) because they are primarily intended to grasp achievability and workspace, respectively.

Table 5. Grouping information for DOF using the Tukey method and a 95% confidence.

Joint number	Grouping information											
20	A											
16	A											
12	A	B										
19	A	B										
8		B	C									
11			C									
3			C									
15				D								
17				D	E							
7					E							
13						F						
18						F						
10						F	G					
14							G					
4								H				
6									I			
9										J		
2											K	
5												L
1												L

To make a comparison between different research findings, it is crucial to determine the status and rank of each hand configuration with respect to others in each study. Generally, based on the comparison between Figure 5(a) and (b), some ranks and statuses are the same. For example, the importance weight of configuration '5.0' in these two is the highest; the relative importance between '2.0' and '2.0c' is the same; or the difference between '3.2' and '3.3' is negligible in both figures. The difference between the ranks between '3.1' and '3.2' is in reverse order in those two figures, or the difference between '3.3' and '4.0' is much wider in Figure 5(a) than in Figure 5(b). These dissimilarities occurred because the referenced study [27] only discussed the grasp achievability, while the current study investigated the quality of each grasp number.

Figure 6(a) and (b) almost have the same configurations in rank. Also, according to Figure 6(a), (b), and (c), especially in two pairs of hand configurations ('3.1' and '3.2'; '4.0' and '4.1'), Figure 6(a) is evidently closer to Figure 6(b). It means that the study [40] mostly took into account workspace, but failed to consider grasp qualities.

3.2. Different hand sections assessment

Some prosthetic hands like SensorHand do not include all five fingers, while some do not consider the last distal joints of fingers. Therefore, it is essential to evaluate the importance of each finger or the functionality loss of prosthetic hands, whose last distal joints are stationary.

The value of each finger can be realized by omitting each of them. The functionality scores of omitting each finger are shown in Figure 7(a). The results demonstrate that the thumb, index, and middle are the most valuable. The little and ring are of the least valuation. However, even omitting the little can reduce the functionality to less than 70%.

Figure 7(b) shows the value of the human hand, the human hand without having the distal phalanges moving, and having only the first phalanges of its fingers. Having only one active phalange in each finger reduces its score by more than 90%.

Figure 7(b) illustrates the impact of omitting independent distal phalange movements. It is also worthwhile to compare prosthetic hands with moving distal phalanges (without independent motor) to those with rigid distal phalanges. As a result, this research chose prosthetic hands called Dextrus v2.0 (moving DIP) and Ada v1.1 (rigid DIP) (these two prosthetic hands are open source and available online according to [41]. However, the authors could not access the content. In both hands, each finger is actuated

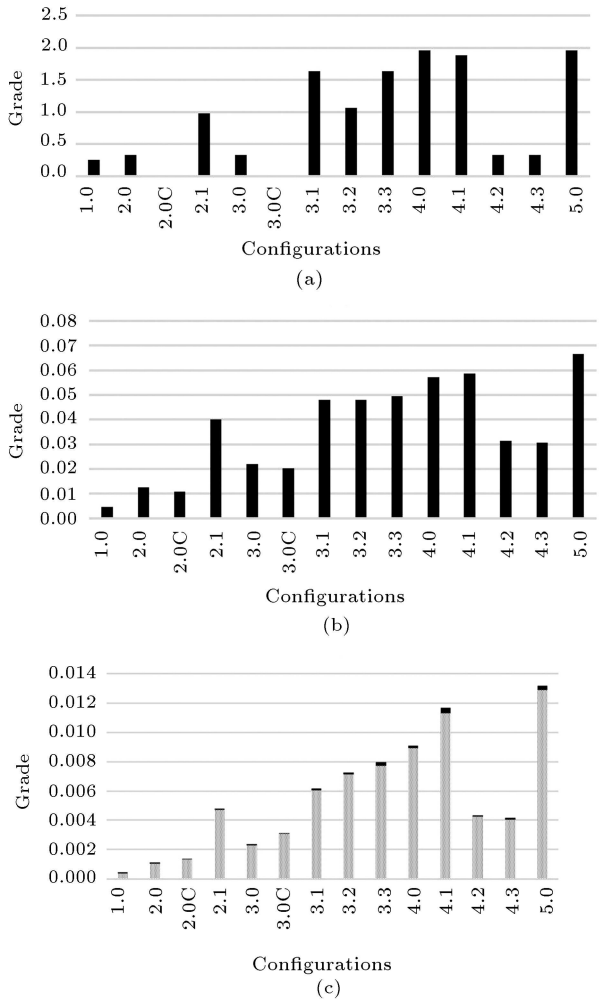

Figure 6. Assessment of hand configurations via (a) ISR Softhand AI [40], (b) workspace grade, and (c) overall functionality grade. In random data. The solid black color indicates a 95% confidence interval.

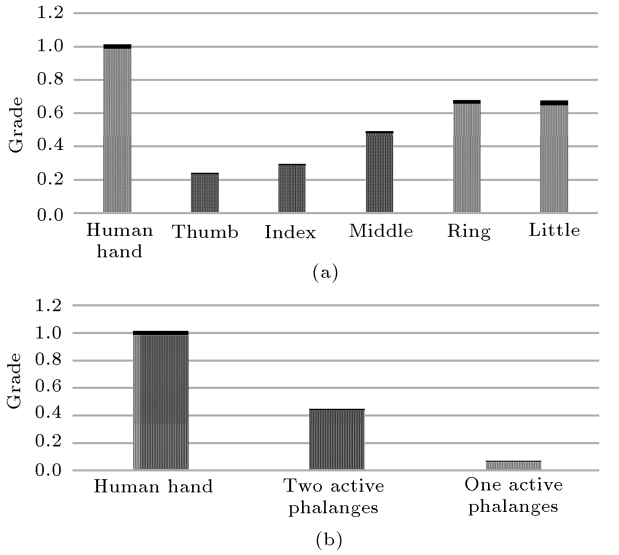

Figure 7. (a) The functionality of the hand after removal of each of the fingers and (b) functionality of the hand related to the number of mobile segments in each of the fingers. The solid black color indicates a 95% confidence interval.

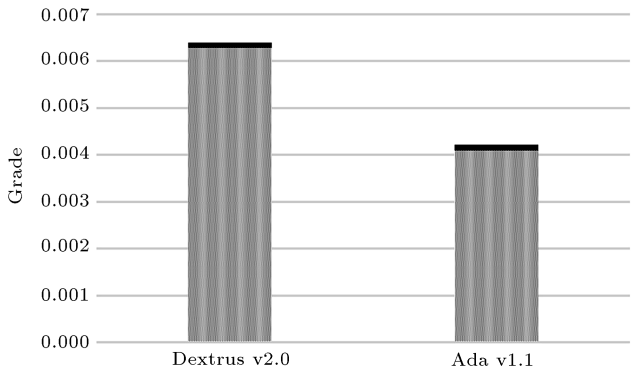

Figure 8. Evaluation of two prosthetic hands. The solid black color indicates a 95% confidence interval.

independently, and only F/E movements are allowed. Furthermore, their CMC joint of the thumb are stationary. The result in Figure 8 depicts that moving DIP is advantageous. However, the Southampton Hand Assessment Procedure (SHAP) results [41] are contrary to this research, because Ada v1.1 has a higher friction coefficient number or less energy loss, which is evident in the slip resistance results [41]. Another reason is that the early F/E of the DIP joints of the Dextrus v2.0 made it difficult to grasp some of the objects. This research does not account for energy loss, transmission ratio, and friction coefficient since they are related to features such as efficiency and materials used in the prosthetic hands and are not related to hand configurations primarily.

Evaluation of each DOF is essential. Table 5 shows grouping information using the Post hoc Tukey method. The general importance level increases from top to bottom of the table. The distal DOFs are of less importance, while the proximal joints, especially the Ab/Ad movement of the first three fingers, are essential. Thumb has the most valuable DOF, which confirms the results given in Figure 7(a). Moreover, the Ab/Ad of the index has the highest value. This is because the index participates in all the grasp types. In addition, Ab/Ad movement generates a force direction that differs from F/E movement, which increases the grasp quality index.

3.3. Optimal configurations via Taguchi method

To obtain an optimal hand configuration, first, it is needed to consider assumptions and constraints. The constraints include having five actuators and nine stationary DOFs. Nine stationary DOFs are chosen according to the least valuable joints from Table 5 (which are 3, 8, 11, 12, 15, 16, 17, 19, and 20). However, the most valuable joints should be driven independently from each other (these joint numbers

Table 6. Results of the Taguchi method. Mean of the main effects. Each level concerns a joint number.

Level	4	7	10	13	14	18
1	0.04309	0.08786	0.10209	0.09285	0.09077	0.08360
2	0.06145	0.08818	0.09652	0.09667	0.08625	0.09213
3	0.11752	0.07725	0.09698	0.08629	0.10031	0.09336
4	0.11013	0.08982	0.08638	0.08861	0.08903	0.09932
5	0.13066	0.11972	0.08087	0.09841	0.09648	0.09443
Delta	0.08757	0.04247	0.02122	0.01213	0.01406	0.01571
Rank	1	2	3	6	5	4

Table 7. Results of the Taguchi method. Signal-to-noise ratios. Each level concerns a joint number.

Level	4	7	10	13	14	18
1	−27.68	−22.05	−20.62	−21.95	−22.12	−22.47
2	−24.94	−22.01	−21.37	−21.00	−22.37	−21.87
3	−18.75	−23.26	−21.52	−22.31	−20.79	−22.04
4	−19.26	−22.30	−22.50	−22.20	−22.24	−20.95
5	−17.71	−18.71	−22.34	−20.88	−20.82	−21.00
Delta	9.97	4.55	1.88	1.44	1.58	1.51
Rank	1	2	3	6	4	5

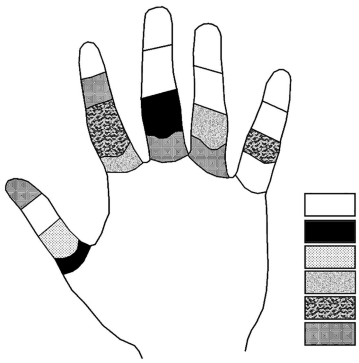

Figure 9. The proposed five actuators hand configuration. White sections are stationary. Others with the same pattern are driven by one actuator. Each finger has four sections that represent its associated DOF. For example, for the index, each section from proximal to distal includes 5, 6, 7, and 8 joint numbers.

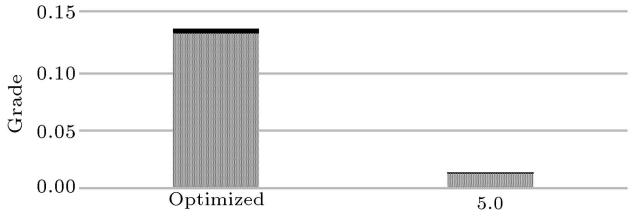

Figure 10. Function score of optimized and '5.0' hand configurations. The solid black color indicates a 95% confidence interval.

are: 1, 2, 5, 6, 9). The last step is to choose which actuators drive each of the six remaining joints, which is done by the Taguchi method. The overall functionality grade was used as an objective function. Results are shown in Tables 6 and 7. A hand configuration is built based on the results, as shown in Figure 9. To determine how much improvement is achieved, the hand configuration of this result and hand configuration '5.0' (Figure 4(c)) are compared via function evaluation in Figure 10. Figure 10 shows that the optimized hand configuration is ten times greater than hand configuration '5.0'. Tables 6 and 7 show the results of the Taguchi method.

4. Discussion

In this study, a number of assumptions are required to use grasp quality as an index for the ability of hand configurations to grasp objects.

In Assumption 1, some DOFs were not taken into consideration and they could be implemented in the future.

Objects were omitted in this research. Alternatively, we can measure the grasp quality with several primitive objects of different sizes and check the results with the current research findings in the future.

Point contacts were considered in this research. If the grasp is force closure in the point contact model in a particular space, the line and surface model grasp is also force closure in that space.

The approximation method for friction cones was employed to implement the convex hull technique. There are also other procedures like changing the nonlinear constraints of friction cone into linear matrix inequalities similar to those given in [42].

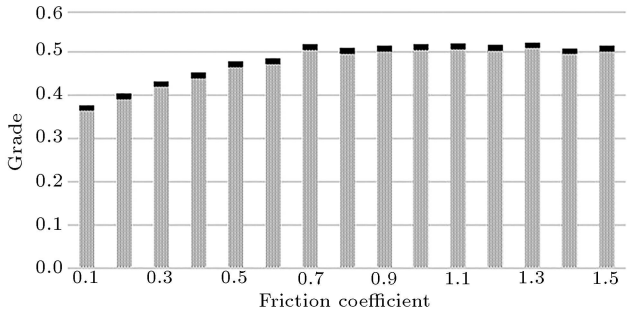

Figure 11. The overall functionality grade of 2 active phalanges in different friction coefficients. The solid black color indicates a 95% confidence interval.

According to Assumption (7), the friction coefficient was 0.4. In Figure 11, the overall functionality score for the hand configuration called 2 active phalanges in Figure 7(b) was measured using different friction coefficients between 0.1 and 1.5. Results indicate that as the friction coefficient increases, the hand configuration score rises until it leveled off at a friction coefficient of 0.7. It means thatgy variances between various hand configurations are reduced as the friction coefficient rises.

Results shown in Figures 7(b) and 8 depict that omitting the DIP joints of the finger and IP joint of the thumb attenuates the functionality. However, deletion of those joints, actuated independently (Figure 7(b)), has greater impact than the dependent ones (Figure 8).

It should be noted that assumptions can be changed, like the contact points of each grasp type, contact model, or human model. The evaluation function can vary as well. In this study, most of the grasp types were examined and had a role in a hand configuration score, but only one specific grasp type or any other combination of grasp types could be used.

5. Conclusion

The weight limitation on prosthetic hands forces designers to omit some parts and Degree of Freedom (DOF) of the human hand to be driven in prosthetic hands. Therefore, this study demonstrated the impact of omitting each DOF, finger, or phalanges on functionality. Results indicated that the most crucial DOF in prosthetic hands was Abduction/Adduction (Ab/Ad) of the thumb's carpometacarpal (CMC) joint and the index's metacarpophalangeal (MCP) joint fingers. Furthermore, the most vital finger was the thumb, while the least vital ones were the ring and the little fingers. Omitting only a finger in prosthetic hands could lead to 70% functionality loss, at least. Finally, this study optimized hand configuration by considering the importance of each DOF and the Taguchi method. This technique generated hand configuration whose functionality was ten times higher than that of the conventional hand configuration '5.0'.

In the future, the proposed optimized hand configuration will be constructed. The proposed functionality algorithm and optimized hand configuration will be examined via various references including [28,41,43].

References

1. Ma'touq, J., Hu, T., and Haddadin, S. "Sub-millimetre accurate human hand kinematics: from surface to skeleton", *Computer Methods in Biomechanics and Biomedical Engineering*, **21**(2), pp. 113–128 (Jan. 2018). DOI: 10.1080/10255842.2018.1425996
2. "https://www.shadowrobot.com/dexterous-hand-series/" .
3. Kaye, R. and Konz, S. "Volume and surface area of the hand", *Proceedings of the Human Factors Society Annual Meeting*, **30**(4), pp. 382–384 (Sep. 1986). DOI: 10.1177/154193128603000417
4. Belter, J.T., Segil, J.L., Dollar, A.M., et al. "Mechanical design and performance specifications of anthropomorphic prosthetic hands: A review", *Journal of Rehabilitation Research and Development*, **50**(5), pp. 599–618 (2013). DOI: 10.1682/JRRD.2011.10.0188
5. Taniguchi, H., Takemoto, N., Yakami, R., et al. "Realistic and highly functional pediatric externally powered prosthetic hand using pneumatic soft actuators", *Journal of Robotics and Mechatronics*, **32**(5), pp. 1034–1043 (2020). DOI: 10.20965/jrm.2020.p1034
6. Nemoto, Y., Ogawa, K., and Yoshikawa, M. "F3Hand: A five-fingered prosthetic hand driven with curved pneumatic artificial muscles", in *2018 40th Annual International Conference of the IEEE Engineering in Medicine and Biology Society (EMBC)*, **2018-July**, pp. 1668–1671 (Jul. 2018). DOI: 10.1109/EMBC.2018.8512692.
7. Controzzi, M., Clemente, F., Barone, D., et al. "The SSSA-MyHand: a dexterous lightweight myoelectric hand prosthesis", *IEEE Transactions on Neural Systems and Rehabilitation Engineering*, **25**(5), pp. 459–468 (May 2017). DOI: 10.1109/TNSRE.2016.2578980
8. Laffranchi, M., Boccardo, N., Traverso, S., et al. "The Hannes hand prosthesis replicates the key biological properties of the human hand", *Science Robotics*, **5**(46), pp. 1–16 (2020). DOI: 10.1126/SCIROBOTICS.ABB0467
9. Nikafrooz, N. and Leonessa, A. "A single-actuated, cable-driven, and self-contained robotic hand designed for adaptive grasps", *Robotics*, **10**(4), p. 109 (2021). DOI: 10.3390/robotics10040109
10. Fajardo, J., Ferman, V., Cardona, D., et al. "Galileo hand: An anthropomorphic and affordable upper-Limb prosthesis", *IEEE Access*, **8**, pp. 81365–81377 (2020). DOI: 10.1109/ACCESS.2020.2990881
11. Leonardis, D. and Frisoli, A. "CORA hand: a 3D printed robotic hand designed for robustness and compliance", *Meccanica*, **55**(8), pp. 1623–1638 (2020). DOI: 10.1007/s11012-020-01188-0

12. Owen, M., Au, C., and Fowke, A. "Development of a dexterous prosthetic hand", *Journal of Computing and Information Science in Engineering*, **18**(1) (Mar. 2018). DOI: 10.1115/1.4038291

13. Ávila-Hernández, P.E. and Cuenca-Jiménez, F. "Design and synthesis of a 2 DOF 9-bar spatial mechanism for a prosthetic thumb", *Mechanism and Machine Theory*, **121**, pp. 697–717 (2018). DOI: 10.1016/j.mechmachtheory.2017.12.001

14. Liow, L., Clark, A.B., and Rojas, N. "OLYMPIC: A modular, tendon-driven prosthetic hand with novel finger and wrist coupling mechanisms", *IEEE Robotics and Automation Letters*, **5**(2), pp. 299–306 (Apr. 2020). DOI: 10.1109/LRA.2019.2956636

15. Hundhausen, F., Starke, J., and Asfour, T. "A soft humanoid hand with in-finger visual perception", *IEEE International Conference on Intelligent Robots and Systems*, pp. 8722–8728 (2020). DOI: 10.1109/IROS45743.2020.9341080

16. Estay, D., Basoalto, A., Ardila, J., et al. "Development and implementation of an anthropomorphic underactuated prosthesis with adaptive grip", *Machines*, **9**(10), pp. 1–21 (2021). DOI: 10.3390/machines9100209

17. Liu, H., Xu, K., Siciliano, B., et al. "The MERO hand: A mechanically robust anthropomorphic prosthetic hand using novel compliant rolling contact joint", *IEEE/ASME International Conference on Advanced Intelligent Mechatronics, AIM*, **2019-July**, pp. 126–132 (2019). DOI: 10.1109/AIM.2019.8868520

18. Smit, G., Plettenburg, D.H., and van der Helm, F.C.T. "The lightweight delft cylinder hand: first multi-articulating hand that meets the basic user requirements", *IEEE Transactions on Neural Systems and Rehabilitation Engineering*, **23**(3), pp. 431–440 (May 2015). DOI: 10.1109/TNSRE.2014.2342158

19. Belter, J.T., Reynolds, B.C., and Dollar, A.M. "Grasp and force based taxonomy of split-hook prosthetic terminal devices", *2014 36th Annual International Conference of the IEEE Engineering in Medicine and Biology Society*, EMBC 2014, pp. 6613–6618 (2014). DOI: 10.1109/EMBC.2014.6945144

20. Mehrkish, A. and Janabi-Sharifi, F. "A comprehensive grasp taxonomy of continuum robots", *Robotics and Autonomous Systems*, **145**, p. 103860 (2021). DOI: 10.1016/j.robot.2021.103860

21. Cutkosky, M.R. "On grasp choice, grasp models, and the design of hands for manufacturing tasks", *IEEE Transactions on Robotics and Automation*, **5**(3), pp. 269–279 (1989). DOI: 10.1109/70.34763

22. Feix, T., Romero, J., Schmiedmayer, H.B., et al. "The grasp taxonomy of human grasp types", *IEEE Transactions on Human-Machine Systems*, **46**(1), pp. 66–77 (Feb. 2015). DOI: 10.1109/THMS.2015.2470657

23. Kyota, F. and Saito, S. "Fast grasp synthesis for various shaped objects", *Computer Graphics Forum*, **31**(2), pp. 765–774 (2012). DOI: 10.1111/j.1467-8659.2012.03035.x

24. Liu, Y., Jiang, L., Yang, D., et al. "Analysis on the joint independence of hand and wrist", *IEEE/ASME International Conference on Advanced Intelligent Mechatronics, AIM*, **2016-Septe**, pp. 31–37 (2016). DOI: 10.1109/AIM.2016.7576739

25. Zarzoura, M., del Moral, P., Awad, M.I., et al. "Investigation into reducing anthropomorphic hand degrees of freedom while maintaining human hand grasping functions", *Proceedings of the Institution of Mechanical Engineers, Part H: Journal of Engineering in Medicine*, **233**(2), pp. 279–292 (2019). DOI: 10.1177/0954411918819114

26. Feix, T., Romero, J., Ek, C.H., et al. "A metric for comparing the anthropomorphic motion capability of artificial hands", *IEEE Transactions on Robotics*, **29**(1), pp. 82–93 (2012). DOI: 10.1109/TRO.2012.2217675

27. Tavakoli, M., Enes, B., Santos, J., et al. "Underactuated anthropomorphic hands: Actuation strategies for a better functionality", *Robotics and Autonomous Systems*, **74**, pp. 267–282 (2015). DOI: 10.1016/j.robot.2015.08.011

28. Mehrkish, A. and Janabi-Sharifi, F. "Grasp synthesis of continuum robots", *Mechanism and Machine Theory*, **168**, p. 104575 (Feb. 2022). DOI: 10.1016/j.mechmachtheory.2021.104575

29. Lippert, L., *Clinical Kinesiology and Anatomy*, FA Davis (2006).

30. Buchholz, B., Armstrong, T.J., and Goldstein, S.A. "Anthropometric data for describing the kinematics of the human hand", *Ergonomics*, **35**(3), pp. 261–73 (Mar. 1992). DOI: 10.1080/00140139208967812

31. Peña-Pitarch, E., Falguera, N.T., and Yang, J. "Virtual human hand: model and kinematics", *Computer Methods in Biomechanics and Biomedical Engineering*, **17**(5), pp. 568–579, Apr. (2014). DOI: 10.1080/10255842.2012.702864

32. Greiner, T.M. "Hand anthropometry of U.S. Army personnel", 1991. [Online]. Available: https://apps.dtic.mil/docs/citations/ADA244533%0Ahttp://oai.dtic.mil/oai/oai?verb=getRecord&metadataPrefix=html&identifier=ADA244533

33. Gracia-Ibáñez, V., Vergara, M., Sancho-Bru, J.L., et al. "Functional range of motion of the hand joints in activities of the International classification of functioning, disability and health", *Journal of Hand Therapy*, **30**(3), pp. 337–347 (Jul. 2017). DOI: 10.1016/j.jht.2016.08.001

34. Coupier, J., Hamoudi, S., Telese-Izzi, S., et al. "A novel method for in-vivo evaluation of finger kinematics including definition of healthy motion patterns", *Clinical Biomechanics*, **31**, pp. 47–58 (2016). DOI: 10.1016/j.clinbiomech.2015.10.002

35. Castelli, G., Ottaviano, E., and Ceccarelli, M. "A fairly general algorithm to evaluate workspace characteristics of serial and parallel manipulators", *Mechanics Based Design of Structures and Machines*, **36**(1), pp. 14–33 (Feb. 2008). DOI: 10.1080/15397730701729478

36. Roa, M.A. and Suárez, R. "Grasp quality measures: review and performance", *Autonomous Robots*, **38**(1), pp. 65–88 (Jan. 2015). DOI: 10.1007/s10514-014-9402-3

37. Miller, A.T. and Allen, P.K. "Examples of 3D grasp quality computations", in *Proceedings 1999 IEEE International Conference on Robotics and Automation (Cat. No.99CH36288C)*, **2**, no. May, pp. 1240–1246 (1999). DOI: 10.1109/ROBOT.1999.772531

38. Tukey, J.W. "Comparing individual means in the analysis of variance", *Biometrics*, **5**(2), p. 99 (Jun. 1949). DOI: 10.2307/3001913

39. Homam, R. and Sayyaadi, H. "Design and optimization of a cybernetics hand", MSc thesis, School of Mechanical Engineering, Sharif University of Technology (2022).

40. Tavakoli, M., Enes, B., Marques, L., et al. "Actuation configurations of bionic hands for a better anthropomorphism index", *Journal of Mechanisms and Robotics*, **8**(4) (Aug. 2016). DOI: 10.1115/1.4032405

41. Andrés-Esperanza, J., Iserte-Vilar, J.L., Llop-Harillo, I., et al. "Affordable 3D-printed tendon prosthetic hands: Expectations and benchmarking questioned", *Engineering Science and Technology, an International Journal*, **31**, p. 101053 (2022). DOI: 10.1016/j.jestch.2021.08.010

42. Han, L., Trinkle, J.C., and Li, Z.X. "Grasp analysis as linear matrix inequality problems", *IEEE Transactions on Robotics and Automation*, **16**(6), pp. 663–674 (2000). DOI: 10.1109/70.897778

43. Kim, J., Iwamoto, K., Kuffner, J.J., et al. "Physically based grasp quality evaluation under pose uncertainty", *IEEE Transactions on Robotics*, **29**(6), pp. 1424–1439 (2013). DOI: 10.1109/TRO.2013.2273846

Biographies

Hassan Sayyaadi (SM'01) received his BSc degree from Amir Kabir University of Technology, MSc degree from Sharif University of Technology, Tehran, Iran, and PhD degree from the University of Tokyo, Japan in 2001, all in Mechanical Engineering. He is currently a Professor at the School of Mechanical Engineering, Sharif University of Technology, Tehran 11155-9567 Iran. His research interests are robotics and mechanisms, intelligent control and applications, smart materials and dynamical systems, and vibrations.

Seyed Reza Homam was born in Liverpool, Northwest England, United Kingdom in 1997. He received a BSc degree in Mechanical Engineering from Ferdowsi University of Mashhad, Mashhad, Iran in 2019. Since September 2019, he has been an MSc student at the Department of Mechanical Engineering at Sharif University of Technology, Tehran, Iran. His research interests include robotics, grasping, multi-body dynamics, and mechanism design.